Bulletin of the Seismological Society of America. Vol. 68, No. 5, pp. 1281–1292, October 1978

THE SOURCE MECHANISM OF THE AUGUST 7, 1966 EL GOLFO EARTHQUAKE

By John E. Ebel, L. J. Burdick, and Gordon S. Stewart

ABSTRACT

The El Golfo earthquake of August 7, 1966 (m_b = 6.3, M_S = 6.3) occurred near the mouth of the Colorado River at the northern end of the Gulf of California. Synthetic seismograms for this event were computed for both the body waves and the surface waves to determine the source parameters of the earthquake. The body-wave model indicated the source was a right lateral, strike-slip source with a depth of 10 km and a far-field time function 4 sec in duration. The body-wave moment was computed to be 5.0 × 10^{25} dyne-cm. The surface-wave radiation pattern was found to be consistent with that of the body waves with a surface-wave moment of 6.5 × 10^{25} dyne-cm. The agreement of the two different moments indicates that the earthquake had a simple source about 4 sec long. A comparison of this earthquake source with the Borrego Mountain and Truckee events demonstrates that all three of these earthquakes behaved as high stress-drop events. El Golfo was shown to be different from the low stress-drop, plate-boundary events which were located on the Gibbs fracture zone in 1967 and 1974.

Introduction

Several studies have been reported in the literature in which long period body-wave form data have been used to model a seismic source (Mikumo, 1971a, b; Burdick and Mellman, 1976; Langston and Butler, 1976; Langston, 1976). Likewise, a number have been based on surface-wave data (Ben-Menahem and Toksoz, 1962, 1963a, b; Kanamori, 1970a, b). Recently Kanamori and Stewart (1976, 1978) have used both types of information to constrain the source models of several earthquakes. In order to fit both the body waves and the relatively longer period surface waves, it is necessary to find a model which accurately represents the behavior of the source over a long time span. While not unique, it is probable that a model which achieves this correctly accounts for the dominant equivalent elastic processes occurring at the source. A relatively simple source model can account for both types of data from some moderate sized strike-slip events such as those along the Gibbs fracture zone (Kanamori and Stewart, 1976) or the Truckee earthquake (Burdick, 1977). For others such as the Borrego Mountain earthquake, a simple model will not simultaneously account for the body- and surface-wave moments (Burdick, 1977). The purpose of this paper is to present the results of a composite surface-wave body-wave study of the August 7, 1966 strike-slip El Golfo earthquake in Sonora, Mexico and to compare its source to those found for the Truckee, Borrego Mountain, and Gibbs fracture zone events.

The El Golfo earthquake is a particularly interesting event to study because of its unique location at the northern end of the Gulf of California. It occurred in a region where the crust is relatively thin, the depth to Moho being only about 20 km (Phillips, 1964). The location of the El Golfo event makes it ideal for a study of its seismic radiation because the available information on the seismic crustal structure near the source (Phillips, 1964) eliminates some of the uncertainties in the body-wave modeling. The near-source structure can be assumed to be known and not changed in the body-wave modeling process.

The origin time and epicenter of the El Golfo earthquake were listed by Sykes (1970) as: 17h36m22.8s UT and 31.72°N, 114.42°W, respectively, with $m_b = 6.3$ and $M_S = 6.3$. The depth was unconstrained. The epicenter was located on the Colorado River delta near the village of El Golfo de Santa Clara in northern Mexico (Figure 1). It occurred on or near a right-lateral strike-slip fault, here called the San Jacinto fault, which runs from Cerro Prieto, an active volcano, into the Gulf of California. A detailed description of this fault is provided by Merriam (1965). Unfortunately, there are no published reports on the effects of this tremor in the epicentral area, although there was a report of ground breaking along this fault in the Colorado delta area (J. Brune, personal communication, 1976). There was a large ($M_L = 7.1$) earthquake in this area in 1934 which had sizable surface displacement (Biehler *et al.*, 1964).

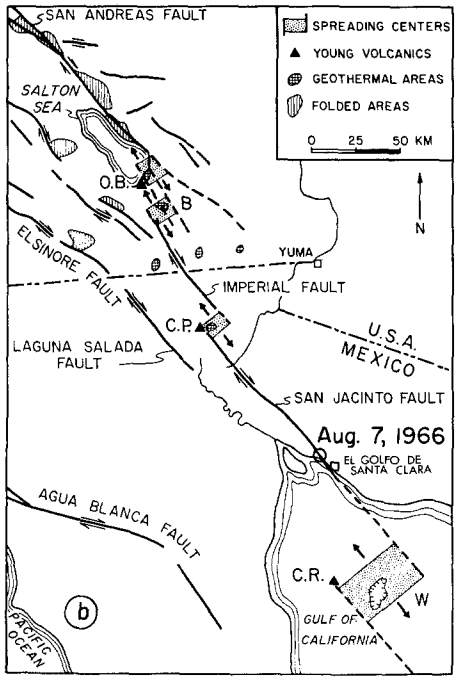

FIG. 1. Location of the El Golfo earthquake on the San Jacinto fault at the mouth of the Colorado River. The interpretation of tectonics is from Elders *et al.* (1972).

TECTONIC SETTING

The El Golfo earthquake occurred in a region where there is a transition from oceanic to continental tectonic features. The Gulf of California is being opened by a series of spreading centers and transform faults which are the northern extension of the East Pacific rise spreading system. In the southern Gulf there is a well developed spreading system, but in the north the details of spreading are unclear. Lomnitz *et al.* (1970) used details of seismicity in the northern Gulf to argue for a series of spreading centers and transform faults running from the Gulf into the Imperial Valley in California. They viewed the San Jacinto fault as a transform fault from the Gulf north to Cerro Prieto. Thatcher and Brune (1971) studied earthquake swarms in the Wagner and Delfin basins in the northern Gulf and concluded that the swarms are related to spreading in these basins.

Henyey and Bischoff (1973) argued from seismic reflection profiles in the northern Gulf that although there is much faulting, the evidence for a spreading center-transform fault system is weak. There are no magnetic stripes anywhere in the Gulf (Larson *et al.*, 1972), although the high sedimentation rate may be obscuring the magnetic lineations. Crustal thickness and seismic velocities are not known in the epicentral region but can be extrapolated from studies in the northern Gulf of California by Phillips (1964) and in the Imperial Valley by Kovach *et al.* (1962). These studies show a crust which is thickest in the Colorado delta region and which thins both north into the Imperial Valley and south into the Gulf of California. The crustal thickness is about 20 km.

Body-Wave Analysis

The body-wave analysis involved computing synthetic seismograms and then comparing them with the data. The synthetic seismograms for P waves are calculated by a series of convolution ($*$) operations according to the formula

$$W = R_{pz}(S*T*Q*I)$$

where W is the vertical displacement at the receiver, R_{pz} is the receiver function, S is the response of the source structure to a point double couple of specified

TABLE 1

Crustal Model for the Source Region

V_p km/sec	V_s km/sec	ρ g/cm^3	Th (km)
1.8	0.5	1.0	1.2
4.0	2.4	1.8	2.3
5.4	3.2	2.4	4.3
6.7	3.9	3.0	16.2
7.8	4.6	3.4	∞

orientation, T is the source-time function, Q is the Earth's attenuation, and I is the instrument response. Expressions for Q, I, and R_{pz} have been derived by Futterman (1962), Hagiwara (1958), and Helmberger (1974), respectively. T is to be determined in the analysis. The procedure used to compute S is the modification of the Thomsen-Haskell layer matrix method by Harkrider (1964) and Fuchs (1966). The details of the method are summarized in Langston (1976). Synthetic seismograms for SH waves were generated in the same way using the appropriate shear-wave receiver function, source structure response, and attenuation operator.

In order to compute the synthetic seismograms, a near-source crustal model, fault-plane solution, time function, and source depth were assumed. These parameters were used to generate synthetic seismograms for 19 teleseismic stations at varying azimuths. The fault-plane solution, time function, and source depth were perturbed by trial and error until the synthetic seismograms best matched the observed data. The crustal model that was used is presented in Table 1. The layers with a P velocity of 6.5 km/sec and 5.0 km/sec are found throughout the northern Gulf province (Phillips, 1964). Above these are two layers of lower velocity which are probably due to sedimentary deposits. The half-space represents the lid with a P velocity of 7.8 km/sec. The initial fault-plane parameters which were used are a slight modification of those given by Sykes (1970). The modification was necessary because the fault planes he published were not orthogonal. The values of $t*$ assumed

in calculating the attenuation operator were 1.3 sec for P waves and 5.2 sec for S waves.

Figures 2, 3, and 4 summarize the body-wave analysis. Figure 2 shows the fault-plane solution for the best fitting model. The focal mechanism of strike 140°, dip

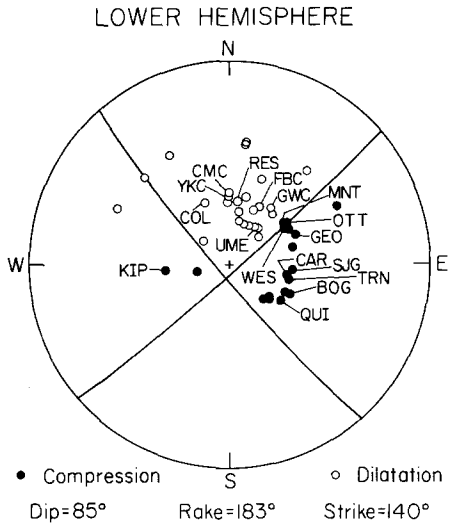

FIG. 2. A focal plot of the P-wave first motions with the locations of stations for which the body waves were modeled. The nodal planes represent those found from the modeling process.

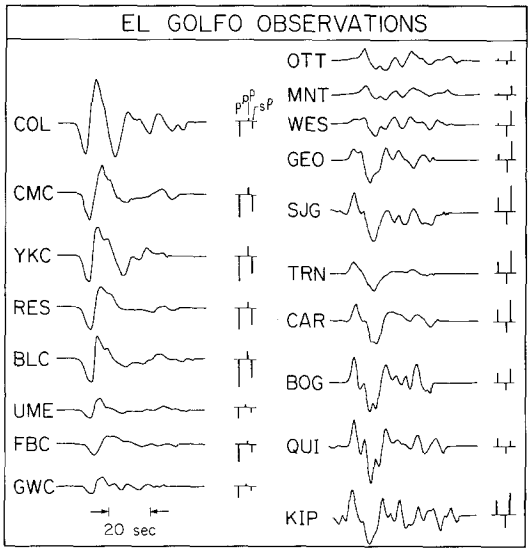

FIG. 3. The first minute or so of the initial P-wave coda as recorded at the stations named in Figure 2. The stick figures to the *right* of each seismogram show the relative polarities, arrival times, and amplitudes of the P, pP, and sP arrivals at that station.

85°, and rake 183° was constrained primarily by the polarity of the P arrivals at the stations in northeastern Canada and by the polarity of the sP arrivals at the stations in South America. In Figure 3, the initial P-wave coda at the stations used in this analysis are presented along with figures indicating the relative amplitudes and arrival times of P, pP, and sP computed from the final source model. Synthetic seismograms computed from this model are presented in Figure 4. The source-time

function for the earthquake was well constrained by modeling OTT and MNT. At these stations the P and pP arrivals were nearly nodal and the first strong arrival was the sP phase. The time function found was a triangle, 4 sec in duration, and the depth of the source was determined to be 10 km. The time-function duration could not be varied by more than 1 sec without significantly affecting the wave forms. Similarly, the depth of the earthquake could not be varied by more than 2 km. The SH waves at four stations, all at roughly the same azimuth and distance from the source, were also modeled using the above parameters and the fit was found to be very good. Hanks *et al.* (1975) also studied the body waves from this earthquake.

Surface-Wave Analysis

The process for computing synthetic surface waves is similar to that for body waves. In this case R_{pz}, S, and T in the above equation are replaced by a function

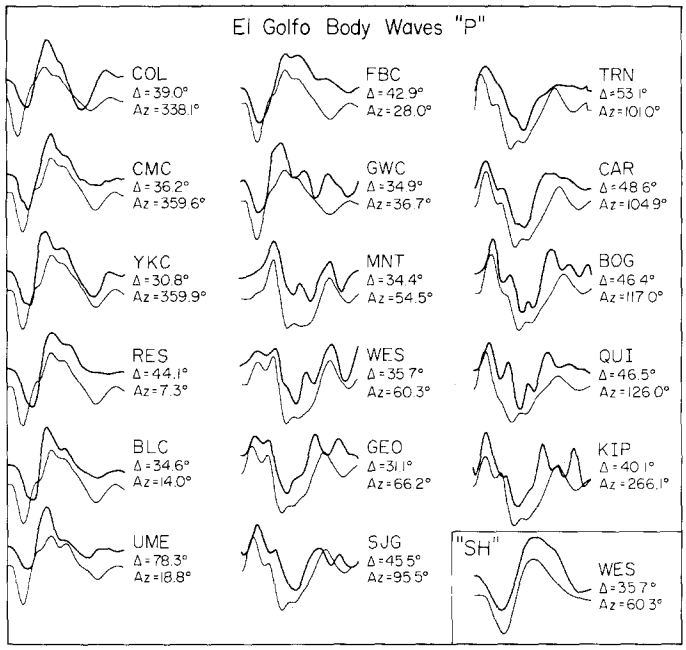

FIG. 4. Data (*top traces*, heavy line) and synthetics (*bottom traces*, light lines) for the P waves at 17 different stations. Data and synthetic for the SH wave at WES are also given. Each trace is 30 sec long.

which describes the response of a spherical earth to a point source. This response is a sum of normal modes which can be found by using the method of Kanamori and Stewart (1976). The synthetic seismograms which are computed can be compared with the data, and the source mechanism and surface-wave moment determined.

Because of the relatively small size of the event, only records from stations closer than 100° from the epicenter could be used. This meant that there were some azimuths at which there were no good records. However, a data set of 25 stations at varying azimuths were chosen. The long-period vertical records were digitized in the appropriate group-velocity window for the Rayleigh waves (R1) and the horizontal records were digitized and rotated for the Love waves (G1). The data were then filtered as described by Kanamori and Stewart (1976) with a short-period cutoff at 35 sec and a long-period roll-off at 300 sec; then they were normalized to a propagation distance of 90° by correcting for anelastic attenuation, geometric spreading, and dispersion. The filtered data are plotted on Figure 5. Finally, using

the source determined from the body waves, a theoretical radiation pattern for the surface waves was generated (Figure 6). The observed Love and Rayleigh waves show a four-lobed pattern consistent with the body-wave mechanism, although the lack of good station coverage to the south and southwest of the source does not provide much information about that part of the radiation pattern. The surface-wave moment for the earthquake was calculated at a number of stations near the radiation maxima for Love and Rayleigh waves and averaged to give a moment of 6.5×10^{25} dyne-cm. These moments were computed at wave periods of about 65 sec for R1 and 70 sec for G1.

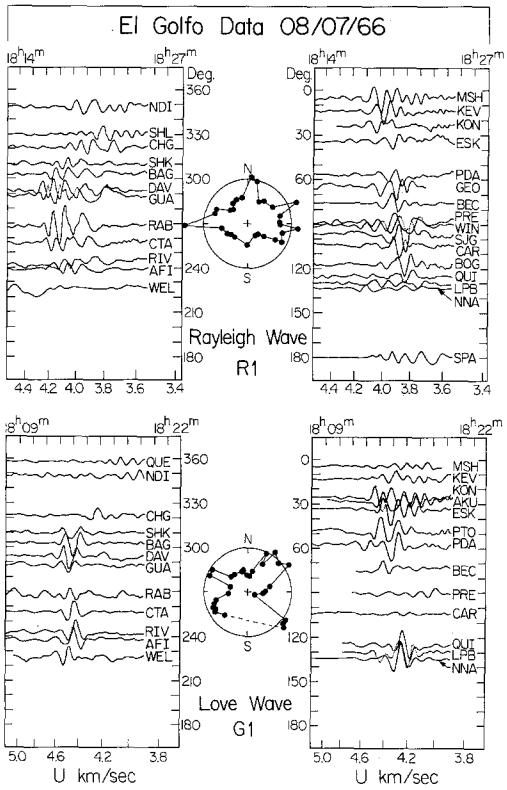

FIG. 5. Observed surface waves, G1 and R1, normalized to a propagation distance of 90°. The rose diagrams show the radiation patterns. The scale at the bottom of each box represents the group velocity U in km/sec.

COMPARISON WITH OTHER EARTHQUAKES

One purpose of this study is to compare the source-time function of this earthquake with those of shallow, strike-slip events which have been modeled in the time domain. Source parameters for the other earthquakes in this comparison, the Borrego Mountain, Truckee, 1967 and 1974 Gibbs fracture-zone events, are given in Table 2. The events are similar in a number of ways. They are all strike-slip earthquakes on nearly vertical faults with depths between 8 and 10 km. The moments of the earthquakes range from 5.7×10^{24} dyne-cm for Truckee to 4.5×10^{26} dyne-cm for the 1974 Gibbs fracture-zone event. The P waves from the events are simple in character due to the fact that, except for the Borrego Mountain, each comes from a single source. The strike-slip source for Borrego Mountain is so much larger and earlier than the later sources that it can be isolated in the records. For all the earthquakes the agreement between the synthetics and observed data is good.

The analysis of the time functions of the earthquakes reveals differences among

them. The Borrego Mountain and Truckee events were modeled with triangular time functions a few seconds in duration. The Gibbs fracture-zone events, on the other hand, were modeled with time functions a couple tens of seconds in duration. The short duration of the El Golfo earthquake makes it appear to be very similar to the other California events. Figure 7 illustrates this dichotomy in time-function character more clearly. The *top left* of the figure shows an observed seismogram

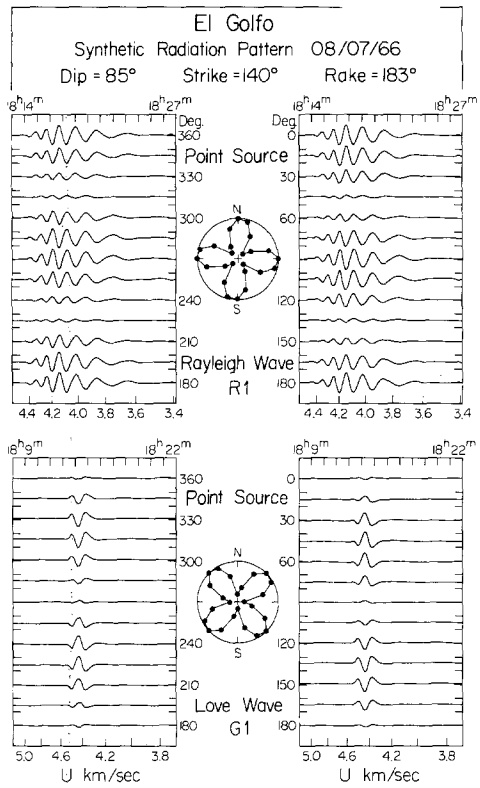

FIG. 6. Synthetic seismograms and radiation patterns for R1 and G1 assuming the focal mechanism and depth found from the *P* waves.

TABLE 2

SOURCE COMPARISON

Event	m_b	M_S	Body Wave M_0 (dyne-cm)	Surface Wave M_0 (dyne-cm)	Depth (km)	Time Function Duration (sec)
El Golfo	6.3	6.3	5.0×10^{25}	6.5×10^{25}	10	4
Borrego Mountain	6.4	6.9	1.1×10^{26}	3.0×10^{26}	8	5
Truckee	5.7	5.9	0.57×10^{25}	1.9×10^{25}	10	3
Gibbs 1967	5.5	6.5	2.0×10^{26}	3.4×10^{26}	10	17
Gibbs 1974	5.8	6.9	5.0×10^{26}	4.5×10^{26}	10	24

from each of the three California earthquakes. The corresponding synthetics are shown beneath each wave form. The focal mechanism plots on the *top right* of the figure show that each station falls at very nearly the same point on its respective radiation pattern. This accounts for the striking similarity between the wave forms for the three events. At this particular station orientation, the direct *P* and *pP* phases are very small precursory arrivals, and the *sP* phase is a large positive arrival which dominates the seismogram. Since the *sP* arrival is so much stronger, its duration can be determined from these particular records with much more accuracy

than from records on which all three arrivals interfere strongly. The triangular time functions which were determined for each earthquake are shown in the *center* of the figure. They too are very similar. The *bottom* of the figure shows the same type of comparison between the El Golfo and Gibbs fracture-zone events. The relative orientations of the stations and the source-to-station distances are again very comparable for the records shown. The wave forms are similar in general shape, but the long-period nature of the Gibbs event is clearly shown by the fact that *P*, *pP*, and *sP* are not identifiable as separate phases, and by the longer total duration of the sum of *P*, *pP*, and *sP* arrivals. Thus, both the wave forms themselves and the time functions from the modeling study indicate that the California earthquakes occurred on a much shorter time scale than the Gibbs fracture-zone event.

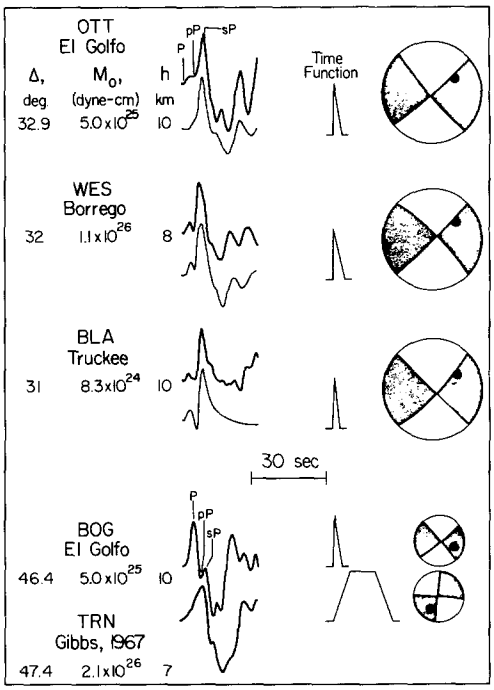

FIG. 7. A comparison of an El Golfo wave form with those from other strike-slip events. Δ is the distance from source to station, M_0 is the moment, and h is the depth of the source. Data is represented by the heavy lines, synthetics by the light lines. The time functions are plotted on the same time scale as the data. At the *right* of each station is the focal mechanism for that earthquake (shaded areas are compression) and the location of the station on the focal sphere.

This time-function difference can be put into a more quantitative form by computing the fault area versus moment for each event. To do this we will adopt the fault model of a circular rupture initiating at a point and growing radially on the fault surface at constant rupture velocity V_r of 0.8β. We will model the total duration T of the time functions shown in the *center* of Figure 7 by assuming the source station geometries on the *right* of Figure 7. The observed pulses can be represented as a convolution of two component pulses which represent the rupture process on the fault and the average dislocation history on the fault. If the rupture process lasts t sec and the average dislocation at a point on the fault lasts q sec, then the total observed time function T duration is given by

$$T = t + q.$$

Under certain assumptions, the rise time on a circular fault can be related to the fault radius a and the shear velocity β by

$$q = \frac{16a}{7\pi\beta}$$

(Geller, 1976). The rupture time is given by

$$t = a\left(\frac{1}{0.8\beta} + \frac{\sin(\delta)}{\beta}\right)$$

TABLE 3

FAULT AREA CALCULATIONS

Event	T Time Function Duration (sec)	q Rise Time (sec)	t Rupture Time (sec)	Fault Area (km^2)
Borrego Mountain	4.5	1.1	3.4	91
Truckee	3.0	0.7	2.3	40
El Golfo	4.0	1.0	3.0	71
Gibbs (1967)	24.0	7.0	10.0	600
Gibbs (1974)	32.0	10.0	12.0	700

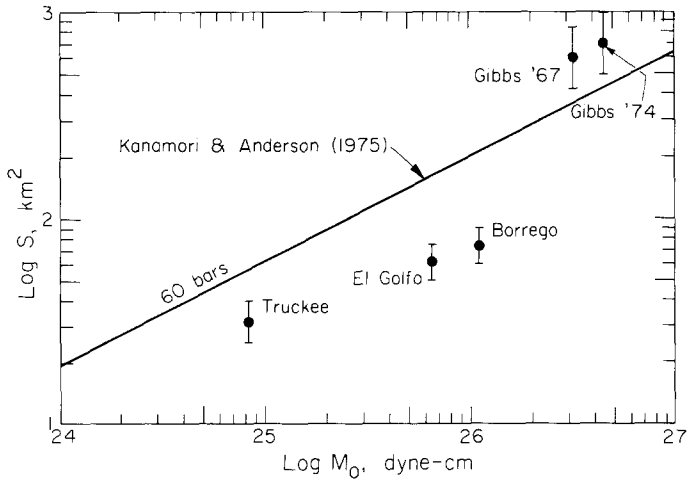

FIG. 8. The relationship of area S and moment M_0 for the different earthquakes in the comparison. The error bars indicate the difference in area assuming a unilateral or a bilateral rupture. The line labeled Kanamori and Anderson (1975) represents the moment-area relation for a circular crack with a stress drop of 60 bars.

where δ is the angle between the normal to the fault plane and the sP ray direction. Thus the fault radius is given by

$$a = \frac{28\pi\beta T}{64 + 7\pi(5 + 4\sin\delta)}.$$

This expression gives values which are consistent with those of Kanamori and Anderson (1975). The results of the calculations are given in Table 3. The rise and rupture time values for the Gibb's fracture-zone events are taken directly from

Kanamori and Stewart (1976) who obtained them by interpreting the different parts of their trapezoidal time functions. As a check, the same values were computed using the above formulism which proved to give similar results.

The observed fault moments and computed fault areas for all the events are plotted in Figure 8. The 60-bar stress-drop line shown in the figure represents an average stress-drop value found for a large number of events by Kanamori and Anderson (1975). It can be seen that the California earthquakes are all high-stress drop events with a smaller than average ratio of log area to log moment, while the Gibbs fracture-zone earthquakes are clearly low-stress drop events.

Conclusions

In this paper the body and surface waves for the El Golfo earthquake were studied together in an attempt to find a single dislocation model which satisfied both. A smooth circular dislocation of about 6 km radius appears to give a satisfactory fit to the data. This model predicts a time pulse of about 4 sec in duration and it matches the observed body- and surface-wave amplitudes if a moment of 6.5×10^{25} dyne-cm is assumed. The focal mechanism is consistent with both types of waves, and the complexity of the *P*-wave forms can be explained by near-source crustal interactions. Neither the *SH* nor surface waves show any unusual complexity. The agreement between the body-wave and surface-wave moments is evidence that the source process ended 4 sec after it started.

Not all earthquake sources appear this simple. Larger events ($M_0 > 10^{27}$ dyne-cm) such as the 1976 Guatemala earthquake (Kanamori and Stewart, 1978) and the 1967 Caracas earthquake (Rial, 1978) were modeled as the sum of several distinct sources. For each of these events the sum of the body-wave moments for the multiple shock equaled the surface-wave moment. On the other hand, the Oroville earthquake, a dip-slip event, had a surface-wave moment which was twice as large as the body-wave moment (Langston and Butler, 1976; Hart *et al.*, 1977). A similar anomaly was found for the Borrego Mountain event (Burdick, 1977). Hart *et al.*, (1977) suggest that this discrepancy may be due to deformations which occurred too slowly to be seen in the body-wave data. This argument, if applied to El Golfo earthquake, indicates that little or no slow deformation accompanied the event.

The El Golfo earthquake was a simple, strike-slip event. It appeared to have a high stress drop like other strike-slip California events and not a low stress drop as observed for two earthquakes along the Gibbs fracture zone. The source duration was approximately 4 sec, and the earthquake had no slow deformation associated with it.

Acknowledgments

The authors wish to thank Don Helmberger for his assistance throughout the course of this study and Hiroo Kanamori for reviewing the manuscript. This study was supported by National Science Foundation Grants EAR76-06619 and EAR76-14262.

References

Biehler, S., R. L. Kovach, and C. R. Allen (1964). Geophysical framework of the northern end of Gulf of California structural province, Marine Geology of the Gulf of California, *AAPG Memoir #3*, 126–146.

Ben-Menahem, A. and M. M. Toksoz (1962). Source mechanism from spectra of long period surface waves 1. The Mongolian earthquake of December 4, 1957, *J. Geophys. Res.* **67**, 1943–1955.

Ben-Menahem, A. and M. N. Toksoz (1963a). Source mechanism from spectra of long period seismic

surface waves: 3. The Alaska earthquake of July 10, 1958. *Bull. Seism. Soc. Am.* **53,** 905–919.

Ben-Menahem, A. and M. N. Toksoz (1963b). Source mechanism from spectra of long period seismic surface-waves 2. The Kamchatka earthquake of November 4, 1952, *J. Geophys. Res.* **68,** 5207–5222.

Burdick, L. J. (1977). Broad-band seismic studies of body waves, *Ph.D. Thesis,* California Institute of Technology.

Burdick, L. J. and G. R. Mellman (1976). Inversion of the body waves of the Borrego Mountain earthquake to the source mechanism, *Bull. Seism. Soc. Am.* **66,** 1485–1499.

Elders, W. A., R. W. Rex, T. Meidav, P. T. Robinson, and S. Biehler (1972). Crustal spreading in southern California, *Science* **178,** 15–24.

Fuchs, F. (1966). The transfer function for *P*-waves for a system consisting of a point source in a layered medium, *Bull. Seism. Soc. Am.* **56,** 75–108.

Futterman, W. I. (1962). Dispersive body waves, *J. Geophys. Res.* **67,** 5279–5291.

Geller, R. J. (1976). Scaling relations for earthquake source parameters and magnitude, *Bull. Seism. Soc. Am.* **66,** 1501–1523.

Hagiwara T. (1958). A note on the theory of the electromagnetic seismograph, *Bull. Earthquake Res. Inst., Tokyo Univ.* **36,** 139–164.

Hanks, T. C., J. A. Hileman, and W. Thatcher (1975). Seismic moments of the larger earthquakes of the Southern California region, *Bull. Geol. Soc. Am.* **56,** 1131–1139.

Harkrider, D. G. (1964). Surface waves in multilayered elastic media I. Rayleigh and Love waves form buried sources in a multilayered elastic half-space, *Bull. Seism. Soc. Am.* **54,** 627–679.

Hart, R. S., R. Butler, and H. Kanamori (1977). Surface-wave constraints on the August 1, 1975, Oroville earthquake, *Bull. Seism. Soc. Am.* **67,** 1–7.

Helmberger, D. V. (1974). Generalized ray theory for shear dislocations, *Bull. Seism. Soc. Am.* **64,** 45–64.

Henyey, T. L. and J. L. Bischoff (1973). Tectonic elements of the northern part of the Gulf of California, *Bull. Geol. Soc. Am.* **84,** 315–330.

Kanamori, H. (1970a). Synthesis of long period surface waves and its application to earthquake source studies—Kurile Islands earthquake of October 13, 1963, *J. Geophys. Res.* **75,** 5011–5027.

Kanamori, H. (1970b). The Alaska earthquake of 1964 long period surface waves and source mechanism, *J. Geophys. Res.* **75,** 5029–5040.

Kanamori, H. and D. L. Anderson (1975). Theoretical basis of some empirical relations in seismology, *Bull. Seism. Soc. Am.* **65,** 1073–1095.

Kanamori, H. and G. S. Stewart (1976). Mode of strain release along the Gibbs fracture zone, mid Atlantic ridge, *Phys. Earth Planet Interiors* **11,** 312–332.

Kanamori, H. and G. S. Stewart (1978). Seismological aspects of the Guatemala earthquake, *J. Geophys. Res.* (in press).

Kovach, R. L., C. R. Allen, and F. Press (1962). Geophysical investigations of the Colorado Delta region, *J. Geophys. Res.* **67,** 2845–2872.

Langston, C. A. (1976). Body wave synthesis for shallow earthquake sources: Inversion for source and earth structure parameters, *Ph.D. Thesis,* California Institute of Technology.

Langston, C. A. and R. Butler (1976). Focal mechanism of the August 1, 1975 Oroville earthquake, *Bull. Seism. Soc. Am.* **66,** 1111–1120.

Larson, P. A., J. D. Mudie, and R. L. Larson (1972). Anomalies and fracture zone trends in the Gulf of California, *Bull. Geol. Soc. Am.* **83,** 3361–3368.

Lomnitz, C., A. F. Mooser, C. R. Allen, J. N. Brune, and W. Thatcher (1970). Seismicity and tectonics of the Northern Gulf of California region, Mexico; preliminary results, *Geophys. Intern.* **10,** 37–42.

Merriam, R. (1965). San Jacinto fault in Northwestern Sonora, Mexico, *Bull. Geol. Soc. Am.* **76,** 1051–1054.

Mikumo, T. (1971a). Source processes of deep and intermediate earthquakes as inferred from long period P and S waveforms 2. Deep-focus and intermediate depth earthquakes around Japan, *J. Phys. Earth* **19,** 303–320.

Mikumo, T. (1971b). Source processes of deep and intermediate earthquakes as inferred from long period P and S waveforms 1. Intermediate-depth earthquakes in the sourthwest Pacific region, *J. Phys. Earth* **19,** 1–19.

Phillips, R. P. (1964). Seismic refraction studies in the Gulf of California, Marine Geology of the Gulf of California, *AAPG Memoir #3,* 90–121.

Rial, J. A. (1978). The Caracas, Venezuela earthquake of July 1967: A multiple source event (submitted for publication).

Savage, J. C. (1966). Radiation from a realistic model of faulting, *Bull. Seism. Soc. Am.* **56,** 577–592.

Sykes, L. R. (1970). Focal mechanism solutions for earthquakes along the world rift system, *Bull. Seism.*

Soc. Am. **60,** 1749–1752.
Thatcher, W. and J. N. Brune (1971). Seismic study of an oceanic ridge earthquake swarm in the Gulf of California, *Geophys. J.* **22,** 473–489.

Division of Geological and Planetary Sciences
California Institute of Technology
Pasadena, California 91125
Contribution No. 2951

Manuscript received September 13, 1977